

## AN INVESTIGATION OF VIBRATIONAL WAVE TRANSMISSION ACROSS COMPLEX JOINTS IN PIPES

S. Bourget, F.J. Fahy

University of Southampton, Institute of Sound and Vibration Research, Southampton, UK

### 1. INTRODUCTION

As part of the development of the Vulcain rocket engine ( Ariane 5's main stage engine ), an SEA (Statistical Energy Analysis ) model has been developed to investigate the dynamic response of the engine to internal and external excitations. This model requires an evaluation of the transmission of vibrational energy between the main components of the engine, and especially, along the pipes connecting them. In order to find out how the vibrational power is transmitted across a complex joint in a fuel line of the engine, and how the internal pressure modifies this transmission, a combination of theoretical models and experiments is being used. This paper describes a method for experimentally evaluating the transmission of vibrational power across a complex joint in a straight pipe and its application to a real rocket engine fuel line. Preliminary results are presented.

### 2. WAVE TRANSMISSION IN SEMI-INFINITE CYLINDRICAL SHELLS VIBRATING *IN VACUO*

Waves travelling in a thin-walled cylindrical shell have axial, circumferential and radial displacement components denoted  $u$ ,  $v$  and  $w$  and can be assumed to take the following form :

$$u = \sum_{n=1}^{\infty} \sum_{s=1}^{\infty} U_{ns} \cos(n(\theta - \theta_{ns})) \exp(-ik_{ns}x + i\omega t + i\pi/2), \quad (1a)$$

$$v = \sum_{n=1}^{\infty} \sum_{s=1}^{\infty} V_{ns} \sin(n(\theta - \theta_{ns})) \exp(-ik_{ns}x + i\omega t), \quad (1b)$$

$$w = \sum_{n=1}^{\infty} \sum_{s=1}^{\infty} W_{ns} \cos(n(\theta - \theta_{ns})) \exp(-ik_{ns}x + i\omega t), \quad (1c)$$

where  $k_{ns}$  is the axial wave number,  $\omega$  is the driving frequency,  $\theta_{ns}$  is the polarization angle and  $x, \theta$  are the cylindrical coordinates (fig.1). *In vacuo* two travelling waves of the same circumferential mode order, at most, can exist at a given frequency ( eg.  $s_{\max} = 2$  ). For a given wave type  $ns$ , the axial, circumferential and radial displacements are linearly related :

$$U_{ns} = R_s W_{ns}, \quad V_{ns} = R_t W_{ns}, \quad (2)$$

# WAVE TRANSMISSION ACROSS COMPLEX JOINTS IN PIPES

The vibrational power carried by this wave is then given by ([1] eq. (24)) :

$$P_{rn} = [\pi E(h/a)^3 / 12(1 - \nu^2)] \omega a W_m^2 [(k_{rn}a)^3 + \nu n^2 (k_{rn}a) + R_r (k_{rn}a)^2 + \nu n R_r (k_{rn}a)] \\ + [\pi E(h/a) / 2(1 - \nu^2)] \omega a W_m^2 [(k_{rn}a) R_r^2 + \nu R_r R_t + \nu R_t] \\ + [\pi E(h/a)(1 - \nu) / 4(1 - \nu^2)] \omega a W_m^2 [n R_r R_t + (k_{rn}a) R_t^2], \quad n > 0 \quad (3)$$

In order to calculate the vibrational power one needs to know four quantities in addition to the pipe material properties ( i.e. Young's modulus,  $E$ , and Poisson ratio,  $\nu$  ). These are the radial displacement amplitude, the axial wavenumber and the two wave amplitude ratios  $R_r$  and  $R_t$  . Although the wave polarization angle is of no importance with regard to the vibrational power, it may be of some help if one wants to understand the mechanisms by which a wave is reflected and transmitted by a discontinuity. Whereas the axial wavenumber and the wave amplitude ratios can be evaluated using theoretical models as described by Fuller and Fahy [1], both the radial wave amplitude and the wave polarization angle must be determined experimentally . This is done by separating each individual wave from the global wave field.

## 3. EXPERIMENTAL WAVE SEPARATION METHOD IN A FINITE LENGTH OF UNIFORM CYLINDRICAL PIPE

### 3.1 Introduction

Waves of a given mode order propagating along a straight uniform cylindrical pipe are partly reflected and transmitted by any discontinuity ( e.g lumped mass, bend, change of material ). They may also be converted into waves of different mode orders. Analysis of the vibrational power transmission and of the wave conversion across a discontinuity therefore requires the identification of each individual propagating wave. Once the global vibrational field has been separated into its different components on both sides of a discontinuity, the total vibrational power transmission ratio,  $\tau_{12}$  , across it, is computed as follows :

$$\tau_{12}(\omega) = \frac{\left( \sum_{n=0}^{\infty} \sum_{m=1}^{\infty} P_{nm}(\omega)_{\text{medium 2}} \right)}{\left( \sum_{n=0}^{\infty} \sum_{m=1}^{\infty} P_{nm}(\omega)_{\text{medium 1}} \right)} \quad (4)$$

where  $P_{ns}(w)$  is the vibrational power carried away by the wave type  $ns$ .

### 3.2 Wave separation principle.

The wave separation is performed in two steps . First, the total vibrational field is decomposed into a sum of all its circumferential mode components using a Fourier decomposition. Second, the incident and reflected waves of every mode order are separated from one another.

## WAVE TRANSMISSION ACROSS COMPLEX JOINTS IN PIPES

3.2.2 The Fourier decomposition. The total propagating radial displacement wavefield has the following form :

$$w(x, \theta) = \sum_{n=0}^{\infty} \sum_{i=1}^{\infty} (W_n^i \exp(-ik_n x) + W_n^r \exp(+ik_n x)) \cos(n(\theta - \theta_n')), \quad (5)$$

where the subscripts  $i$  and  $r$  denote the incident and reflected waves. In the low frequency case, where at most one wave of a given mode order propagates, the total wave field can be decomposed as follows:

$$(W_n^i \exp(-ik_n x) + W_n^r \exp(+ik_n x)) \cos(n(\theta_n - \theta_n')) = \frac{1}{\pi} \int_0^{2\pi} w(x, \theta) \cos(n(\theta - \theta_n')) d\theta, \quad (6)$$

This is achieved practically by measuring the radial displacement at  $N$  different locations around the circumference of the pipe at a given position,  $x$ , along its axis (fig. 2). Equation (6) then becomes :

$$(W_n^i \exp(-ik_n x) + W_n^r \exp(+ik_n x)) \cos(n(\theta_n - \theta_n')) = \frac{1}{\pi} \sum_{j=1}^J w(x, \theta_j) \cos(n(\theta_j - \theta_n')) (2\pi / J), \quad (7)$$

Since the wave polarization,  $\theta_n$ , is *a priori* unknown, this process is repeated for different values of  $\theta_n'$  until  $\cos(n(\theta_n - \theta_n')) = 1$ . At this stage, both the wave polarization and a combination of the incident and reflected waves are known for every mode order.

3.2.2 The axial separation. After applying the Fourier decomposition at two different locations  $x_1$  and  $x_2$  along the axis of the pipe, one can separate the incident and reflected waves in the following manner. The Fourier decompositions gave the system :

$$(W_n^i \exp(-ik_n x_1) + W_n^r \exp(+ik_n x_1)) \cos(n(\theta_n - \theta_n')) = \frac{1}{\pi} \sum_{j=1}^J w(x_1, \theta_j) \cos(n(\theta_j - \theta_n')) (2\pi / J), \quad (8)$$

$$(W_n^i \exp(-ik_n x_2) + W_n^r \exp(+ik_n x_2)) \cos(n(\theta_n - \theta_n')) = \frac{1}{\pi} \sum_{j=1}^J w(x_2, \theta_j) \cos(n(\theta_j - \theta_n')) (2\pi / J), \quad (9)$$

Using Flügge's equations for the free vibrational motion of a thin-walled shell [2], it is possible to calculate the theoretical dispersion curves and the wave amplitude ratios  $R_a$  and  $R_r$  as shown by Fuller and Fahy [1]. Once  $k_n$  is known, the radial displacement amplitudes  $W_n^i$  and  $W_n^r$  can be determined by simply inverting the system above. After applying this method to every mode order over the complete frequency range of interest, one can evaluate the total vibrational power carried away by the different waves using eq. (3).

### 3.3 Practical procedure

$N$  transfer functions between the radial displacement and the excitation force are measured at regularly spaced locations around several rings, situated at known positions along the axis of the pipe. Two rings are theoretically sufficient, however, if only one wave of a given mode order propagates at the frequency of interest. For each pair of rings, the wave separation is performed. It is then possible to use the redundant results to check the accuracy of the radial wave amplitudes by observing their scatter.

### WAVE TRANSMISSION ACROSS COMPLEX JOINTS IN PIPES

#### 3.4 Discussion

3.4.1 Advantages : (i) Unlike other works ( Pavic [3], de Jong and Verheij [4] ) where either simplified theoretical or experimental dispersion curves are used, this method relies on an accurate theoretical model. (ii) The polarization angle of the different circumferential modes is determined and can be used to understand the wave transmission across complex discontinuities.

3.4.2. Limitations : (i) The use of this method is limited only to parts of the pipe where no near field is present. (ii) If one is interested in higher order mode transmission, a large enough number of measurements must be taken around every ring in order to avoid aliasing during the Fourier decomposition. (iii) This method requires that the waves have a radial component large enough to be measured by conventional light weight accelerometers. The method is therefore not suitable for the  $n=0$  circumferential mode, in which the displacement is mainly axial at low frequency.

### 4. MEASUREMENT OF THE VIBRATIONAL POWER TRANSMISSION ACROSS A GIMBALED JOINT

#### 4.1 Description of the system pipe plus joint

The piece of pipework on which the experiment is carried out comprises typical components of a Vulcain engine fuel line. The gimbaled joint, across which the transmission of vibrational power is to be measured, connects two straight sections of cylindrical pipe ( fig. 2 ). It is heavy and stiff but can deform around its two articulation axes, thus allowing the forces to be transmitted across it, unlike the bending moments. The thickness to radius ratio of the pipes is 0.04 and the total system length is 12 times the pipe diameter.

#### 4.2 Objectives of the experiment

The aim of this experiment is to evaluate the transmission of vibrational power across the joint when one section of the pipe is radially excited by a point force in the low frequency range 500-5000 Hz ( ring frequency of the pipe : 27 kHz). Simultaneously, possible mode conversion is to be investigated. To do so, the transmission of the  $n=1,2,3$  and 4 circumferential modes will be separately evaluated.

#### 4.3 Experimental arrangement

The experimental arrangement is shown in fig. 3 . In order to limit the amplitude of the axial resonances, some damping is added at both pipe terminations ( damping tapes and thin damped beams ). Four rings, each having eight measurement points, are used on both sections of the pipe.

#### 4.4 Results

4.4.1 Wavefield decomposition. In order to assess the quality of the wave field decomposition the incident and reflected waves have been separated at two different locations along the axis of the pipe ( pairs of rings x1x2 and x3x4 - pipe 2 for  $n=1$  and 2, pipe1 for  $n=3$  ). Figures 4,5 and 6 show that the magnitudes of the incident wave amplitudes match fairly well over a large part of the frequency range. Discrepancies between 2500 and 2750 Hz and above 4700 Hz are due to poor quality measurements and will not be taken into account in the further analysis. This method for separating individual higher order mode waves from a reactive wavefield therefore appears satisfactory.

## WAVE TRANSMISSION ACROSS COMPLEX JOINTS IN PIPES

4.4.2 Vibrational power transmission. Figure 7 shows the vibrational power transmission ratios of individual modes. One can see large variations in these ratios over the frequency range of interest. They are likely to be due to the complex dynamics of the joint. The vibrational power carried by circumferential  $n=1$  and 2 modes transmits much better across the joint than that of the  $n=3$  mode. A drop in the quality of the measurements occurs at the cut-off frequency of the  $n=3$  mode ( 2350 Hz ), this could explain the high power transmission ratio ( +10 dB ) of the  $n=1$  mode observed at this frequency. The total power transmission ratio ( fig. 8 ) displays as well large variations ( from -20 dB to 0 dB ) with frequency.

### 5. CONCLUSION

A method for measuring vibrational power flow along a uniform cylindrical thin-walled pipe is described here. It is based on the use of both theoretical and experimental results and requires only several simple radial acceleration measurements to be made on the surface of the pipe. An application of this method to the evaluation of the power transmission across a complex joint between pipes is presented. Preliminary results are shown here : further experiments are being carried out to evaluate the reliability of the method.

### 6. ACKNOWLEDGMENTS

The authors gratefully acknowledge the Société Européenne de Propulsion and the Centre National d' Etudes Spatiales for financing this work within the R&T programme.

### 7. REFERENCES

1. C.R. FULLER and F.J. FAHY 1982 Characteristics of wave propagation and energy distributions in cylindrical elastic shells filled with fluid. *Journal of Sound and Vibration* **81**, 501-518.
2. A.W. LEISSA 1973 Vibration of shells. *NASA SP-288*.
3. G. PAVIC 1992 Vibroacoustical energy flow through straight pipes. *Journal of Sound and Vibration* **154**, 411-429.
4. C.A.F. de JONG and J.W. VERHEIJ 1992 Measurements of energy flow along pipes. *Proceedings of the second international congress on recent developments in air- and structure-borne sound and vibration*, 577-584.

WAVE TRANSMISSION ACROSS COMPLEX JOINTS IN PIPES

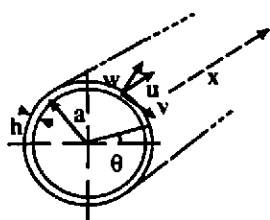


Figure 1: Geometry

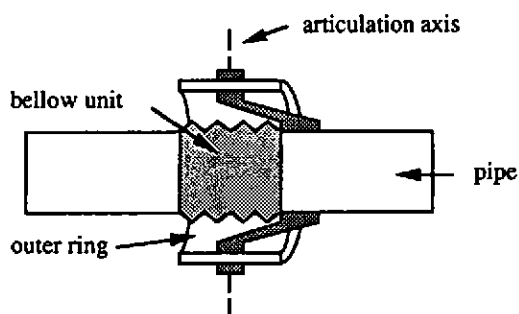


Figure 2 : Section through the Gimballed Joint

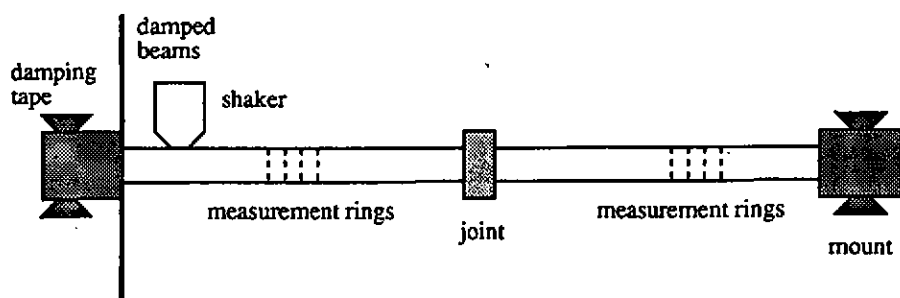


Figure 3: Experimental Set-Up

WAVE TRANSMISSION ACROSS COMPLEX JOINTS IN PIPES

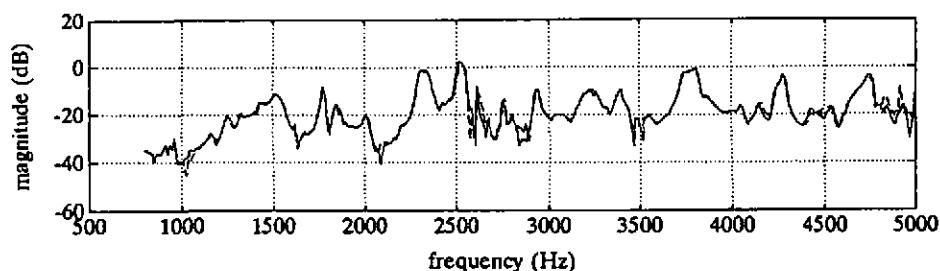


Figure 4 : Magnitudes of the transmitted wave amplitudes ( $n = 1$ )  
( ---- : rings 1 and 2; --- : rings 3 and 4 )

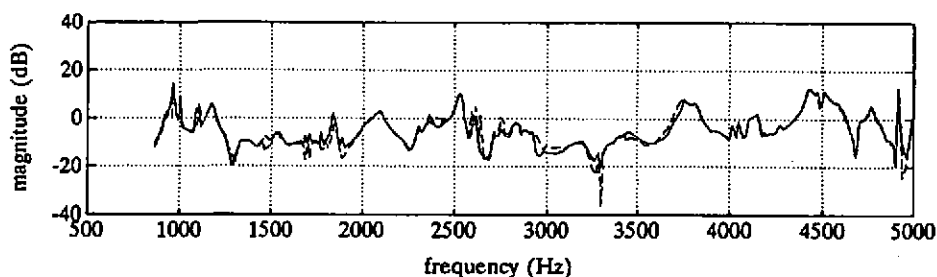


Figure 5 : Magnitudes of the transmitted wave amplitudes ( $n = 2$ )  
( ---- : rings 1 and 2; --- : rings 3 and 4 )

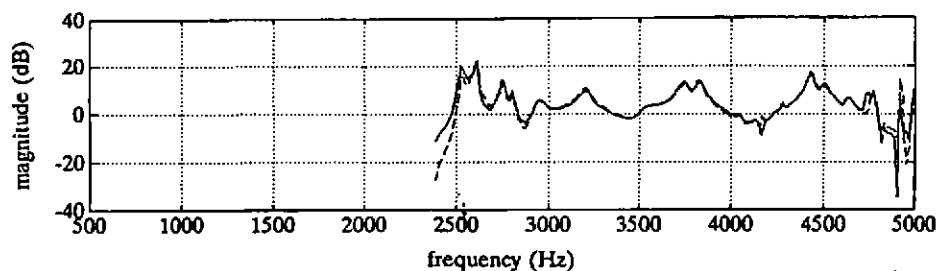


Figure 6 : Magnitudes of the incident wave amplitudes ( $n = 3$ )  
( ---- : rings 1 and 2; --- : rings 3 and 4 )

WAVE TRANSMISSION ACROSS COMPLEX JOINTS IN PIPES

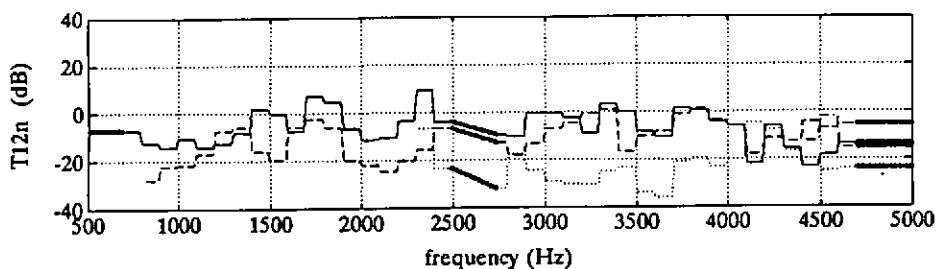


Figure 7 : Modal power transmission ratios  
( ..... : n=1, - - - - : n=2, - . - . : n=3, - - - - : n=4; ##### : region of low confidence )

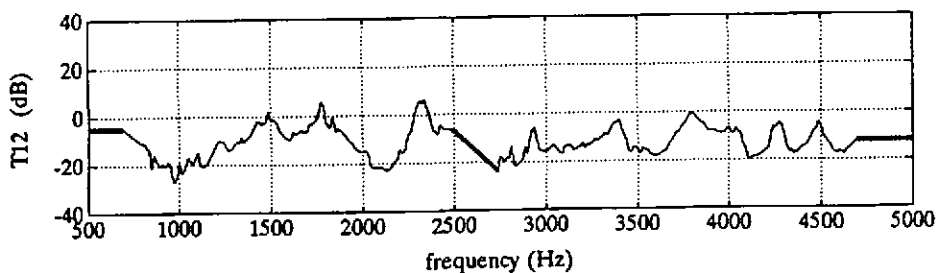


Figure 8 : Total vibrational power transmission ratio across the joint  
( ##### : region of low confidence )